Characterization of ultrathin films by laser-induced sub-picosecond photoacoustics with coherent extreme ultraviolet detection

Qing Li[1], Kathleen Hoogeboom-Pot[1], Damiano Nardi[1], Chris Deeb[2] , Sean King[2], Marie Tripp[2], Erik Anderson[3], Margaret M. Murnane[1], and Henry C. Kapteyn[1]

1) Department of Physics, JILA, and NSF Engineering Research Center in Extreme Ultraviolet Science and Technology, University of Colorado and NIST, Boulder, CO 80309-0440

2) Intel Corp. 2501 NW 229th Ave, Hillsboro, OR, 97124

3) Center for X-Ray Optics, Lawrence Berkeley National Laboratory, Berkeley, CA 94720

ABSTRACT

Photoacoustic spectroscopy is a powerful tool for characterizing thin films. In this paper we demonstrate a new photoacoustic technique that allows us to precisely characterize the mechanical properties of ultrathin films. We focus an ultrafast laser onto a nano-patterned thin film sample, launching both surface acoustic waves (SAWs) and longitudinal acoustic waves (LAWs). Coherent extreme ultraviolet pulses are then used to probe the propagation dynamics of both the SAWs and LAWs. The resulting photoacoustic signal on both short (picosecond) and long (nanosecond) time scales yields important information. In the first 100ps, a fast oscillation followed by an echo signal corresponds to LAWs traveling inside the nanostructures and the thin film, from which the LAW velocities in the two materials can be extracted. On longer time-scales, SAW oscillations are observed. By combining the measured SAW frequency with the wavelength (determined by the nanostructure period) the SAW velocity can be accurately determined, even for very short wavelength surface acoustic waves with very small penetration depths. Using this technique, the elastic properties, including the Young's modulus and Poisson ratio for the thin film, can be obtained in a single measurement, this technique can be extended to sub-10nm thin films.

KEYWORDS:

metrology, photoacoustic, surface acoustic wave, longitudinal acoustic wave, thin film, extreme ultraviolet, high harmonic generation, Young's modulus, Poisson's ratio

I. INTRODUCTION

Thin film technology is widely employed in a variety of fields, from nanotechnology to aerospace, where it is used for example for conductive and insulating layers in electronic devices, or for multilayer optical mirrors and filters. Advances in nanotechnology demand commensurate advances in nanoscale characterization techniques. Conventional spectroscopic and scanning techniques usually measure the chemical and electrical properties of a thin film, but cannot determine the mechanical properties. Brillouin scattering can measure both longitudinal and transverse acoustic waves, but the interpretation remains indirect and rather complex. Moreover, the intensity of the scattered light is very weak, making characterization strongly dependent on the accuracy of the required attenuation measurements[1].

Laser-based photoacoustic characterization, which measures the ultrasonic response of a film after heating with a pulsed laser, provides an effective alternative way to measure the elastic properties of thin films including the Young's modulus

Metrology, Inspection, and Process Control for Microlithography XXVI, edited by Alexander Starikov,
Proc. of SPIE Vol. 8324, 83241P · © 2012 SPIE · CCC code: 0277-786X/12/$18 · doi: 10.1117/12.916866

that characterizes stiffness and Poisson's ratio which corresponds to the ratio of the size change in the direction perpendicular to the applied force compared with the compressed length in the direction of the force. Acoustic waves can thus be used to nondestructively characterize density, elastic properties, and thin film thickness— provided we monitor the complete dynamics of the acoustic wave propagation. Approaches to metrology based on photoacoustic generation are already widely used. A picosecond laser pulse incident on an absorption layer or opaque metal film will launch a longitudinal wave into a transparent dielectric[2, 3] and interfacial reflections monitored with another laser pulse can be used to determine the Young's modulus. However, this method only measures the longitudinal acoustic velocity. Thus, the Young's modulus can be extracted only by assuming a value of Poisson's ratio, which can vary as the material dimensions shrink to submicron size[4]. A mechanical approach using an AFM tip to generate nanoscale acoustic waves can also be used[1], but the delicate procedure and strong influence of the substrate make it difficult to obtain consistent results using this method.

In this work, we use ultrafast laser heating of a nano-patterned structure deposited onto the film to launch ultra-short wavelength surface acoustic waves (SAWs) and longitudinal acoustic waves (LAWs) simultaneously. The SAWs propagate with a penetration depth proportional to a fraction of the SAW wavelength Λ_{SAW}, making them sensitive to the mechanical properties of the thin film[5, 7]. The LAWs travel into the material, reflecting from any interfaces present. When both waves are fully confined within a thin film and their dynamics are directly observed, the 3D mechanical properties of the film can be precisely characterized, including both the Young's modulus and Poisson's ratio. By using coherent extreme-ultraviolet light, we can probe very short-wavelength SAWs, allowing us to extend this technique to <<10 nm dimensions.

II. SAMPLE AND EXPERIMENTAL SETUP

In this experiment we characterized a 100 nm-thick amorphous hydrogenated silicon carbide (a-SiC:H) film deposited on a silicon substrate, with a density of 1.55g/cm^3 and nominal Young's modulus of 30 GPa. The thickness of the film was measured using ellipsometry, and the Young's modulus was measured by nano-indentation[6]. To generate very short-wavelength SAWs[7, 8], we deposited a 1D nanopatterned Ni grating onto the film. The gratings were 10 nm high, with line-widths of 52, 111, 212, 361 and 514 nm (verified using an SEM) and periods of 156, 305, 600, 1090, 1527 nm.

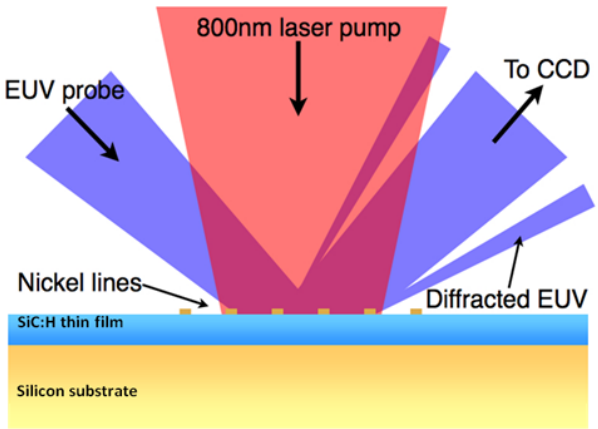

Figure 1: Schematic illustration of experimental geometry for photoacoustic metrology on a nano-patterned thin film sample. The film is 100nm thick a-SiC:H, and the patterned nickel grating has widths vary from 52 nm to 514 nm, and period from 156 to 1527 nm.

Figure 1 shows the sample geometry. In this experiment, we the output of a Ti:sapphire amplifier system (3kHz, 30fs, 2mJ, 800nm) is split into pump and probe beams. The pump beam is sent through a computer-controlled translation stage and loosely focused onto the sample to launch the acoustic waves. The probe pulse is focused into an argon-filled hollow waveguide to generate coherent ultrafast extreme ultraviolet (EUV) beams[9], with wavelength centered at 30nm. The intensity of the EUV beams reflected and diffracted from the sample is recorded as a function of pump-probe time delay

to obtain the photoacoustic response. Since the acoustic waves distort the surface, the diffraction efficiency of the grating varies. Thus, the grating structure plays a role both in creating and observing the ultrashort SAWs.

III. TIME-RESOLVED SIGNAL

In this experiment, the pump pulse causes a sudden thermal expansion of the Ni nano-grating, inducing a stress at the nanostructure/thin-film interface and launching transverse and longitudinal acoustic waves. Longitudinal waves travel from the nanostructure into the thin film and then into the substrate; in this process the LAWs can be partly reflected at the both nanostructure/thin-film and thin-film/bulk interface. The transverse SAWs travel in a surface layer of depth proportional to the acoustic wavelength. Figure 2 shows a typical acoustic response on both short and long time-scales.

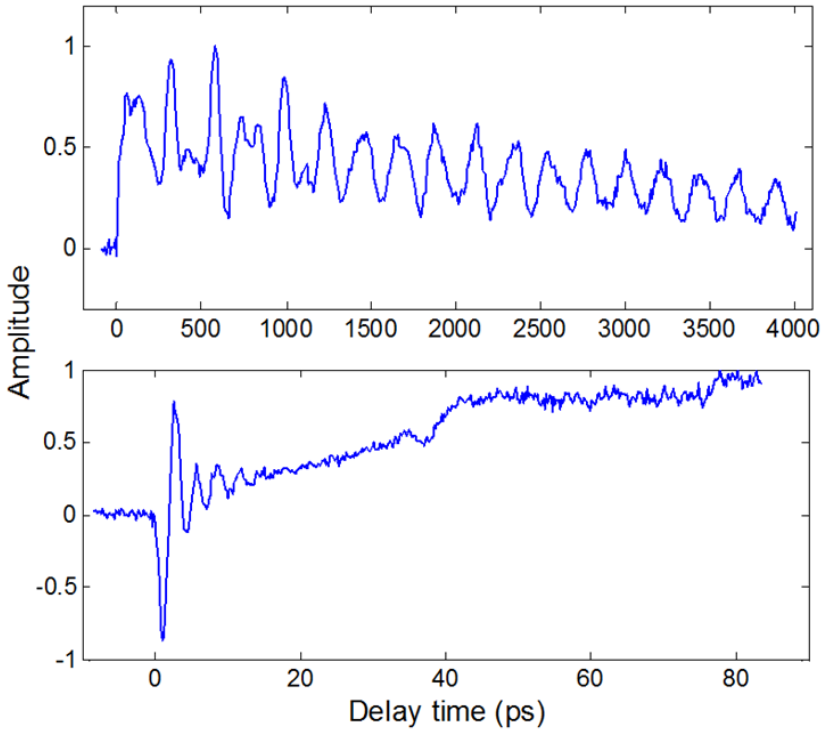

Figure 2: Time-resolved EUV signal as a function of pump-probe time delay, in the case of a 100 nm thick film with a 1090nm period overlaid nickel grating. The short time scale curve (top) reveals both the longitudinal acoustic oscillation inside the 15nm thick nano-grating and the longitudinal wave echo from the underlying 100nm film, while the long time scale result (bottom) shows multi-frequency surface acoustic waves.

Since the grating thickness is 10nm while the period is much longer, the frequency of the LAW is higher than of the SAW (the SAW wavelength corresponds to the period of the grating). This allows the SAW and the LAW response to be easily separated in time. Figure 2 shows the typical transient change in the EUV diffraction signal as a function of pump-probe delay time on the 100nm-thick film sample capped with a 1090nm period nickel grating. The two graphs show the same data set, with the top panel corresponding to the initial (LAW) response.

In the top panel of Fig. 2, the initial fast oscillation in the first 10 ps results from longitudinal acoustic waves propagating entirely within the nickel nanostructures. An echo signal around 38ps can also be seen, which is due to the longitudinal wave propagating into the film and reflecting at the film/substrate interface. The bottom panel of Fig. 2 shows slower oscillations corresponding to the SAWs[7]. Superimposed on these SAW oscillations is a fast rise and slow fall in the overall signal that results from thermal expansion of the Ni lines, and subsequent thermal dissipation from the nanostructure through the thin film into the bulk[10].

IV. LONGITUDINAL ACOUSTIC WAVE RESPONSE

The surface and longitudinal acoustic waves are distinguished both in their direction of travel and in their time scales, which allows us to analyze them independently. Short timescale scans for all five different grating show the same fast oscillation around zero delay time as well as the echo signal at about 38ps. Figure 3 re-plots the top curve of Fig. 2, the dynamic signal at short time scales, as shown in blue line. We can remove the thermal expansion background by curve fitting with a single exponential function (purple line) to extract the acoustic-only signal (green). Then we use a sinusoidal wave with exponential damping to fit to the oscillation (red), obtaining the acoustic wave frequency of 330 ± 6 GHz. We can also more-clearly see the echo signal at 38ps in the background subtracted signal.

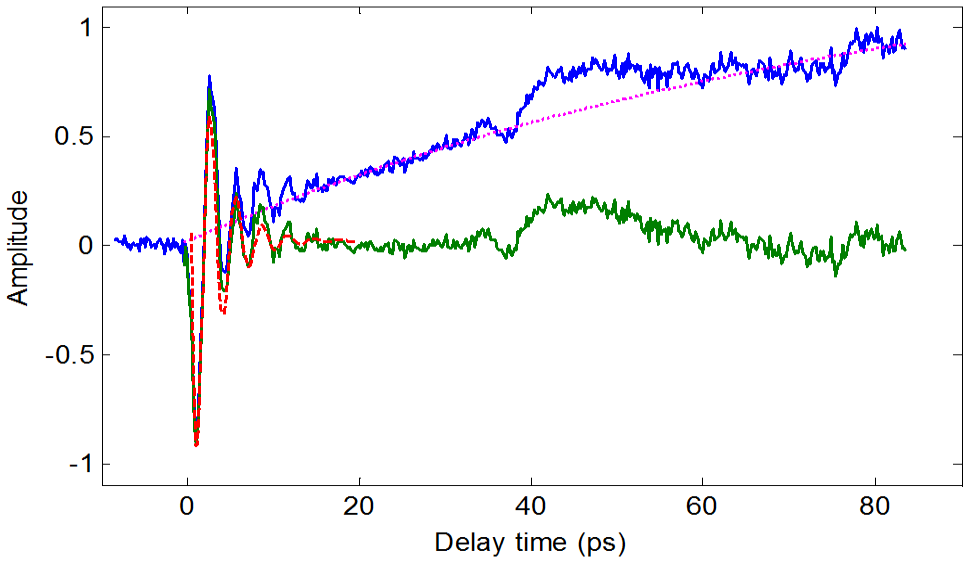

Fig. 3: Precise characterization of the longitudinal frequencies in a 100 nm thin film capped by a 350 nm period grating. The rising part is subtracted from original time-resolved scan signal (blue) using an exponential fit (purple), thus extracting the acoustic signal (green). The first 20 ps of the damped oscillation is fit (red) to obtain the LAW frequency.

Knowledge of the film and grating thickness allows us to determine the LAW speed for both Ni and the thin film as $v_{LAW\text{-}Ni} = 2hf_{LAW} = 2 \cdot 10nm \cdot 330GHz = 6596m/s$, and $v_{LAW\text{-}film} = 2 \cdot 100nm/38ps = 5263m/s$.

These measured values have relatively large uncertainty (±10%) because fast damping limits the total number of oscillations, therefore limiting the frequency resolution. This measured LAW velocity in nickel is consistent with values from other sources, while the LAW velocity in the thin film is sensitive to the mechanical properties and density of the film.

V. SURFACE ACOUSTIC WAVES

Surface acoustic waves are induced by the stress associated with thermal expansion of the laser-heated nano-grating, and these SAWs propagate along the surface. Their frequencies are determined by wavelength and velocity as

$v_{SAW} = \Lambda_{SAW} \cdot f_{SAW}$, where Λ_{SAW} is the SAW wavelength set by the nano-grating period P, and v_{SAW} depends on the elastic properties and density of the material. When the SAW is concentrated near an interface of two or more different materials, the effective phase velocity depends on the elastic properties and material density at both sides of the interface.

SAW propagation is primarily confined within a layer of thickness ζ corresponding to ($\zeta_{SAW} \sim \Lambda/\pi$), as shown in Figure 4. Therefore, the SAW velocity is very sensitive only to the materials within ζ_{SAW} from the surface. Given our a-SiC:H thin

film sample, the overlaid grating periods were chosen to cover three regimes: (1) when the penetration depth is much larger than the film thickness ($\zeta_{SAW} \gg T$), SAWs propagate primarily in the silicon substrate and the frequency is determined by Young's modulus and density of the silicon substrate, as shown purple dotted line in Figure 4; (2) when $\zeta_{SAW} \sim T$, the elastic properties of both the a-SiC:H thin film and silicon substrate play important role in determining the SAW velocity; and (3) when SAWs are confined mainly within the thin film ($\zeta_{SAW} \ll T$), the SAW frequency reflects the mechanical properties of the thin film, as shown green dashed line in Figure 4. Note that the strongest SAW has a wavelength Λ equal to the period P of nano-grating. However, higher-order oscillations with wavelength a fraction of the grating period are also excited, and these higher frequency waves have shorter penetration depths. In the case of intermediate SAW period (in our case the 600 nm period), the fundamental SAW oscillation is sensitive to the silicon substrate, while the second-order SAWs are confined within the thin film.

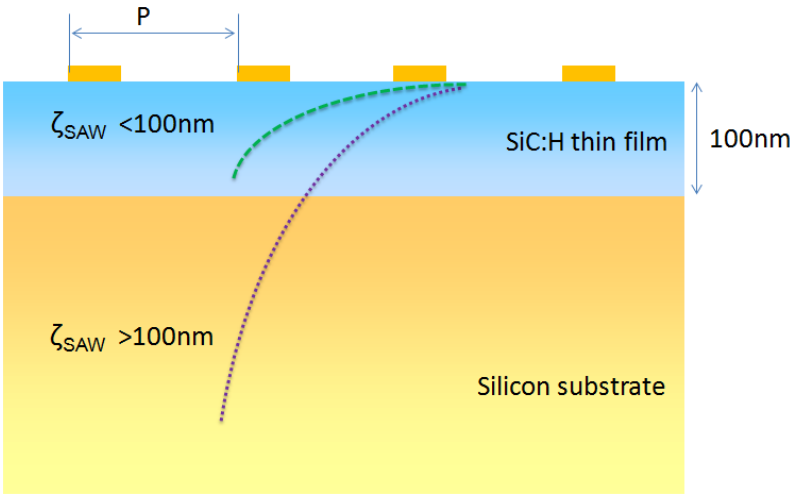

Fig. 4: Illustration of SAW localization at different wavelength Λ, as the penetration depth $\zeta_{SAW} \sim \Lambda/\pi$. For large gratings, the SAWs propagate mainly in the silicon substrate (purple dotted line); for small gratings, the SAWs are confined completely within the film (green dashed line); and for the intermediate period of gratings, the first-order SAW has longer penetration depth that reach down to the substrate while the second-order SAW is localized within the film, resulting in the distinct value of measured velocities.

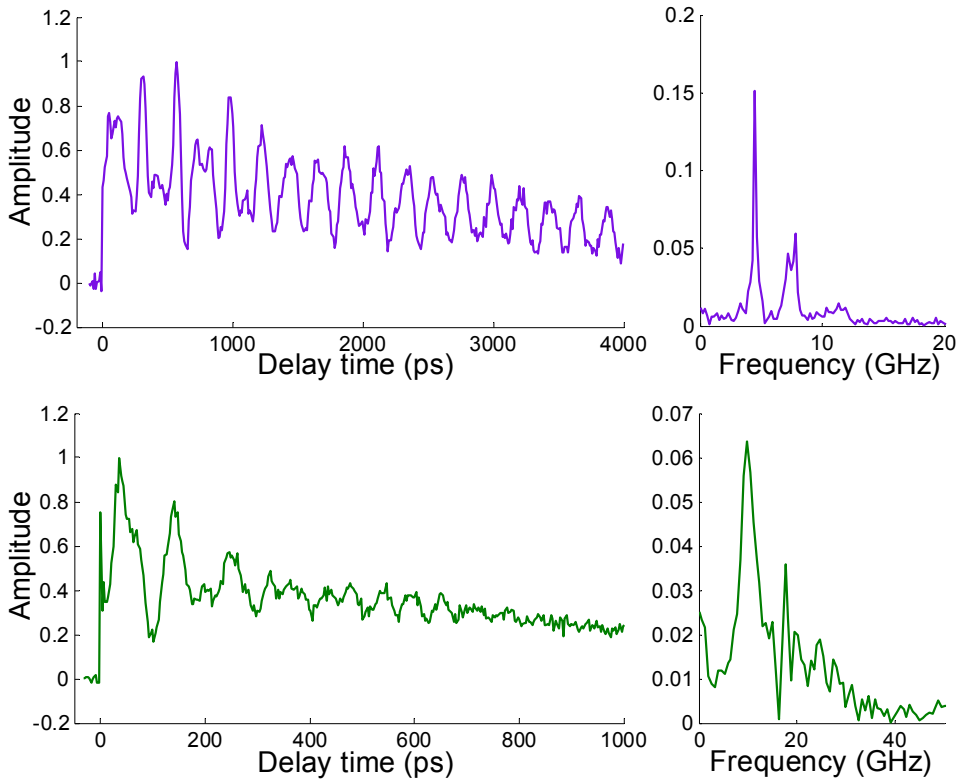

Fig. 5: Time-resolved dynamics of surface acoustic wave oscillations for 1090nm (top) and 305nm (bottom) grating periods. Raw data are shown on the left, while their Fourier transform spectra are on the right. In both cases we see a strong peak at the fundamental frequency, but also see peaks that correspond to higher-order (i.e. shorter wavelength/ higher frequency) excitations.

SAW wavelength (nm)	**v_{SAW} from 1st order (m/s)**	**v_{SAW} from 2nd order (m/s)**
1527	4900±190	4410±380
1090	4900±180	4520±360
600	4250±150	3360±300
305	3060±153	2740±306
156	2800±156	2900±312

Table 1: Measured SAW velocities for nano-patterned thin film samples of five different grating periods. Both fundamental and second order SAWs are included. Higher SAW velocities are measured when the SAW wavelength is large enough so that the SAW propagates primarily in the silicon substrate, while the slowest velocities correspond to SAWs confined within the softer thin film.

Figure 5 shows two typical data sets for surface acoustic waves. A Fourier transform is used to extract the first and second order frequencies of these oscillations. Based on dispersion equation of SAWs, the v_{SAW} for different grating periods and oscillation orders are calculated, and the results are presented in Table 1. For large grating periods (i.e. long wavelength), a SAW velocity of ≈ 4900 m/s is measured, which matches the expected speed in silicon. This observation verifies our prediction that the SAW propagates primarily in the silicon substrate for large grating periods (long SAW wavelengths), and validates the reliability of SAW measurement. For short grating periods, the measured velocity decreases. For periods of 600 nm, the velocities from the 1st order and 2nd order SAWs are clearly different, which illustrates the high sensitivity of SAW measurement. Finally, for periods of 156 nm, when the SAWs is localized at the surface in the nanostructure and underlying thin film, the extracted SAW velocity falls by ~2x to 2800m/s, consistent with a softer material, i.e. a thin film with lower Young's modulus than the silicon substrate.

We note that the patterned nickel nanostructure has a minor effect on the SAW velocity measurement: it slows down the SAW propagation velocity by introducing additional acoustic impedance (also known as mass loading effect) [11, 12]. This contribution can be removed by effective mass-loading approximation[12], or by finite element simulation[13], as discussed in details in our previous experiments[7,8]. Using a finite element simulation method here, we can remove the effect from nickel nanostructures at the smallest gratings, and extract the SAW velocity in the thin film of $\mathrm{v_{SAW}} = 2997\mathrm{m/s}$.

VI. ELASTIC PROPERTIES

If the thin film sample is isotropic, the values of both longitudinal and transverse velocities can be used to completely determine the elastic tensor of a material as $c_{44} = \rho v_T^2$, and $c_{11} = \rho v_{LAW}^2$. Here v_T is the velocity of the transverse acoustic wave, which is simply related to SAW velocity by $v_{SAW} = v_T/\sigma$, where σ is the Landau factor and equals 0.92 in our case. Using $\mathrm{v_{SAW}} = 2997\mathrm{m/s}$ and $v_{LAW-film} = 5263 m/s$, we can calculate the elastic tensor element c_{11} and c_{44}.

The elastic tensor can be used to determine the mechanical properties of a material[14], since the Young's modulus can be calculated from $E = c_{44}\left(\frac{3c_{11}-4c_{44}}{c_{11}-c_{44}}\right)$, and Poisson's ratio is given by $\nu = \frac{c_{11}-2c_{44}}{2(c_{11}-c_{44})}$.

Using a density of $1.55 \times 10^3\ kg/m^3$, we calculate that the Young's modulus is $E = 36 \pm 3\ GPa$, which is consistent with the nominal value, while Poisson's ratio is calculated to be $\nu = 0.24 \pm 0.07$.

VII. CONCLUSION

In summary, we demonstrate a new photoacoustic technique to characterize the mechanical properties of ultrathin films. By focusing an ultrafast laser onto a nano-patterned thin film sample, SAWs and LAWs are launched simultaneously, and measured using coherent EUV pulses. Both the frequencies and velocities of the SAWs and LAWs of the thin film are extracted. As a result, the elastic properties of 100nm thin films are obtained. This approach can easily be extended to measurements of sub-10 nm films.

REFERENCES

[1] Link, A., Sooryakumar, R., Bandhu, R. S., and Antonelli, G. A. "Brillouin light scattering studies of the mechanical properties of ultrathin low-k dielectric films". J. of Appl. Phys., 100, 013507 (2006).

[2] Thomsen, C., Grahn, H. T., Maris, J. H., and Tauc, J. "Picosecond interferometric technique for study of phonons in the Brillouin frequency range", Optics Communication, 6, 55 (1986).

[3] Grahn, H., T., Maris, H. J., and Tauc, J., "Picosecond ultrasonics", IEEE J. of Quantum Electronics, 25, 12 (1989).

[4] Greaves, G., Greer, A., Lakes, R., and Rouxel, T., "Poisson's ratio and modern materials", Nature Materials, 10, 823 (2011).

[5] Auld, B. A., Acoustic Fields and Waves in Solids, Vol. I, Wiley-Interscience, New York (1973).

[6] Stan, G., King, S., and Cook, R., "Elastic modulus of low-k dielectric thin films measured by load-dependent contact-resonance atomic force microscopy", Journal of Material Research, 24, 2960 (2009).

[7] Siemens, M., Li, Q., Murnane, M., Kapteyn, H., Yang, R., Anderson, E., and Nelson, K. "High-frequency surface acoustic wave propagation in nanostructures characterized by coherent extreme ultraviolet beams", Appl. Phys. Lett., 94, 093103 (2009).

[8] Li, Q., Hoogeboom-Pot, H., Nardi, D., Murnane, M., and Kapteyn, H., Siemens, M., Anderson, E., Hellwig, O., Dobisz E.,Gurney, B., Yang, R., and Nelson, K., "Generation and Control of Ultrashort-Wavelength Surface Acoustic Waves at Nano-interfaces", submitted.

[9] Popmintchev, T., Chen, M., Arpin, P., Murnane, M., and Kapteyn, H., "The attosecond nonlinear optics of bright coherent X-ray generation", Nature Photonics, 4, 822 (2010).

[10] Siemens, M., Li, Q., Yang, R., Nelson, K. Anderson, E., Murnane, M., and Kapteyn, H., "Quasi-ballistic thermal transport from nanoscale interfaces observed using ultrafast coherent soft X-ray beams", Nature Materials, 9, 26 (2010).

[11] Auld, B. A., Acoustic Fields and Waves in Solids, Vol. II, Wiley-Interscience, New York, pages 275-283 and 302-309 (1973).

[12] Datta, S., and Hunsinger, B., "Reduction of surface acoustic wave grating impedance and velocity perturbations via buried bimetallic electrode geometries", J. Appl. Phys., 50, 5661 (1979).

[13] Nardi, D., Travagliati, M., Siemens, M., Li, Q., Murnane, M., Kapteyn, H., Ferrini, G., Parmigiani, F., and Banfi, F., "Probing Thermomechanics at the Nanoscale: Impulsively Excited Pseudosurface Acoustic Waves in Hypersonic Phononic Crystals", Nano Letter 11, 4126 (2011).

[14] Li, Q., Study of Nanoscale Phonon Dynamics using Ultrafast Coherent Extreme Ultraviolet Beams. PhD thesis, University of Colorado at Boulder (2011).